

Oblique sub- and super-harmonic Bragg resonance of surface waves by bottom ripples

MOHAMMAD-REZA ALAM, YUMING LIU,
AND DICK K. P. YUE†

Department of Mechanical Engineering, Center for Ocean Engineering, Massachusetts Institute of Technology, Cambridge, MA 02139, USA

(Received 15 July 2009; revised 16 October 2009; accepted 17 October 2009)

We consider a class of higher order (quartet) Bragg resonance involving two incident wave components and a bottom ripple component (so called class III Bragg resonance). In this case, unlike class I/II Bragg resonance involving a single incident wave and one/two bottom ripple components, the frequency of the resonant wave, which can be reflected or transmitted, is a sum or difference of the incident wave frequencies. In addition to transferring energy across the spectrum leading to potentially significant spectral transformation, such resonances may generate long (infragravity) waves of special importance to coastal processes and engineering applications. Of particular interest here is the case where the incident waves are oblique to the bottom undulations (or to each other) which leads to new and unexpected wave configurations. We elucidate the general conditions for such resonances, offering a simple geometric construction for obtaining these. Perturbation analysis results are obtained for these resonances predicting the evolutions of the resonant and incident wave amplitudes. We investigate special cases using numerical simulations (applying a high-order spectral method) and compare the results to perturbation theory: infragravity wave generation by co- and counter-propagating incident waves normal to bottom undulations; longshore long waves generated by (bottom) oblique incident waves; and propagating–standing resonant waves due to (bottom) parallel incident waves. Finally, we consider a case of multiple resonance due to oblique incident waves on bottom ripples which leads to complex wave creation and transformations not easily tractable with perturbation theory. These new wave resonance mechanisms can be of potential importance on continental shelves and in littoral zones, contributing to wave spectral evolution and bottom processes such as sandbar formation.

Key words: scattering, stability, surface gravity waves

1. Introduction

Resonant wave-bottom interactions affect the development of the wave spectrum in the coastal regions and continental shelves (e.g. Hara & Mei 1987; Mei, Hara & Naciri 1988), modify bottom sandbars (e.g. Heathershaw & Davies 1985; Yu & Mei 2000*b*) and generate waves that are of concern, for example, to ocean vehicles moored in shallow basins (e.g. Renaud *et al.* 2008), and possibly to microseismic noise (e.g. Babcock, Kirkendall & Orcutt 1994).

† Email address for correspondence: yue@mit.edu

We consider sub- and super-harmonic third-order (quartet class III) Bragg resonance involving three surface waves and one bottom ripple component in a general three-dimensional context. This problem differs from class I/II Bragg resonances which obtain at second/third order involving two monochromatic surface waves and one/two bottom components (e.g. Davies & Heathershaw 1984; Naciri & Mei 1988; Liu & Yue 1998 where different classes of Bragg resonance are discussed; Ardhuin & Herbers 2002; Madsen & Fuhrman 2006) in that the resonant wave is sub- or super-harmonic in frequency (equal to the difference or sum of the two incident wave frequencies). Furthermore, in the special case of collinear waves and bottom ripples, the resonant wave in class III resonance can be transmitted or reflected whereas only the latter obtains in class I and II resonances.

Class I and II Bragg resonance of surface waves due to bottom undulations has been measured (e.g. Elgar, Raubenheimer & Herbers 2003); studied experimentally (e.g. Heathershaw 1982; Davies & Heathershaw 1984; Hara & Mei 1987; Guazzelli, Rey & Belzons 1991); theoretically using regular (Davies 1982) and multiple-scale (Mei 1985) perturbation, mild slope equation (Kirby 1986; Porter & Porter 2001); and numerically using direct simulations (Liu & Yue 1998).

In this work, we focus on third-order class III Bragg resonances in the general three-dimensional case. Of special interest are the conditions under which these obtain and the resulting wave configurations that may be of importance. We discuss the general resonant conditions and introduce a simple geometric construction for obtaining these (§2). §3 presents a multiple-scale analysis for the evolution of the resonant and incident wave amplitudes. Perturbation predictions are useful for isolated resonance conditions, but, for general wave and bottom environments for which possibly many frequency/wavenumber components are present and hence multiple resonances occur, direct numerical simulations are effective. In §4, we present numerical results, using the direct simulation method of Liu & Yue (1998), for a number of illustrative scenarios. The results compare well with the perturbation predictions.

These scenarios show that, under realistic but suitable incident wave conditions in the presence of periodic bottom ripples, class III sub- and super-harmonic resonance can result in the generation of wave systems distinct and not obtained in class I and II Bragg reflection. Of particular interest is the possibility of new sub-harmonic transmitted and reflected shore-normal (§4.1) and shore-parallel (§4.2) resonance waves that can be of significantly longer wavelengths (and lower frequencies) than the incident waves. When longshore incident waves (normal to the bottom ripples) are present, class III resonance can result in super-harmonic standing waves parallel to and of the same wavelength as the bottom ripple (§4.3). Under normal conditions, incident waves may contain multiple frequencies (and be oblique to the bottom ripples). We consider such a case in §4.4, and show how three-dimensional multiple class III resonances can lead to highly complex wave systems. These features of nonlinear wave-bottom resonant interactions may have important implications to mooring of ships and near-shore structures, and to coastal processes such as sandbar formation.

2. Resonance condition

We consider the irrotational motion of a homogeneous inviscid incompressible fluid with a free surface ignoring surface tension. We assume constant (mean) water depth, h , with bottom ripples of wavenumber k_b and incident waves of wavenumber k and frequency ω , both of relatively mild slope so that perturbation theory applies.

The linearized dispersion relationship can be written as $\mathcal{D}(\mathbf{k}, \omega) \equiv \omega^2 - gk \tanh kh = 0$, where $k = |\mathbf{k}|$, or simply $\mathcal{F}(\omega) = k$. From perturbation analysis (see e.g.

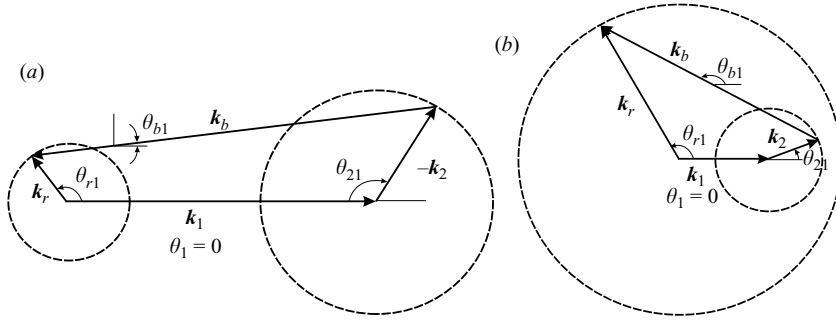


FIGURE 1. Geometric construction for conditions for (a) subharmonic and (b) superharmonic class III quartet Bragg resonance.

Mei 1985; Liu & Yue 1998), at the second order, an incident wave of wavenumber \mathbf{k}_1 is resonantly reflected by bottom ripples \mathbf{k}_b if the so-called class I Bragg resonance condition, $\mathcal{F}(\omega_1) = |\mathbf{k}_1 \pm \mathbf{k}_b|$, is satisfied. The resonant reflected wave is then given by $(\mathbf{k}_r, \omega_r) = (\mathbf{k}_1 \pm \mathbf{k}_b, \omega_1)$. Class I Bragg resonance has been studied extensively (e.g. Davies 1982; Mei 1985; Kirby 1986; Liu & Yue 1998; Arduin & Magne 2007).

At the third order, resonance interactions occur among quartet of propagating waves and bottom components. We classify the case involving two surface $(\mathbf{k}_1, \mathbf{k}_r)$ and two bottom wavenumber $(\mathbf{k}_{b1}, \mathbf{k}_{b2})$ components as class II Bragg resonance; and that involving three surface $(\mathbf{k}_1, \mathbf{k}_2, \mathbf{k}_r)$ and one bottom wavenumber (\mathbf{k}_b) components as class III Bragg resonance (see Liu & Yue 1998; Madsen & Fuhrman 2006). Class II resonance is a direct extension of class I to the third order, with \mathbf{k}_b replaced by $\mathbf{k}_{b1} \pm \mathbf{k}_{b2}$ in the resonance condition, i.e. $\mathcal{F}(\omega_1) = |\mathbf{k} \pm \mathbf{k}_{b1} \pm \mathbf{k}_{b2}|$, with the reflected wave given by $(\mathbf{k}_r, \omega_r) = (\mathbf{k}_1 \pm \mathbf{k}_{b1} \pm \mathbf{k}_{b2}, \omega_1)$.

Our present interest is class III Bragg resonance which has the general condition: $\mathcal{F}(\omega_1 \pm \omega_2) = |\mathbf{k}_1 \pm \mathbf{k}_2 \pm \mathbf{k}_b|$, resulting in a resonant wave $(\mathbf{k}_r, \omega_r) = (\mathbf{k}_1 \pm \mathbf{k}_2 \pm \mathbf{k}_b, \omega_1 \pm \omega_2)$. Note that, in contrast to class I and II where $\omega_r = \omega_1$, the resonant wave frequency now equals to the sum and difference of the two incident wave frequencies.

We offer, in figure 1, simple geometric constructions for class III Bragg resonance for general finite depth for separately the sub- and super-harmonic cases. For the subharmonic case (figure 1a): for given \mathbf{k}_1 and \mathbf{k}_2 (without loss of generality we assume $\mathbf{k}_1 = k_1 \hat{i}$ and $k_1 = |\mathbf{k}_1| > |\mathbf{k}_2| = k_2$), a bottom component \mathbf{k}_b that connects the end of $\mathbf{k}_1 - \mathbf{k}_2$ to the resonance circle (circle of radius $k_r = |\mathbf{k}_r|$ centred at the origin) forms a class III Bragg quartet among $\mathbf{k}_1, \mathbf{k}_2$ and \mathbf{k}_r (in figure 1, θ_{ij} is the angle between \mathbf{k}_i and \mathbf{k}_j). A similar graphical solution obtains for superharmonic class III resonance (figure 1b). In figure 1(a, b) the radius of the \mathbf{k}_r circle decreases/increases as k_2 increases in such a way that the \mathbf{k}_2 circle (of radius k_2 centred at the tip of \mathbf{k}_1) is always outside/inside the \mathbf{k}_r circle. Note that in either figures, since \mathbf{k}_b has no frequency, cases with θ_{b1} and $\pi \pm \theta_{b1}$ have identical solutions. From figure 1(a, b), it is also seen that θ_{r1} can in general vary between 0 and 2π , i.e. the resonant wave can be reflected *or* transmitted.

3. Perturbation solution

Perturbation solution for class I and II Bragg reflection are now well known (e.g. Mei 1985; Kirby 1986). The extension to class III is somewhat straightforward (see Liu & Yue 1998; Madsen & Fuhrman 2006, for the solution in a special case).

For completeness, we outline here the general class III multiple-scale perturbation solution.

In a class III Bragg resonance three surface waves exchange energy via a bottom topography components. To obtain the time evolution (similar argument can be given for the spatial evolution), consider three surface waves travelling on water depth h over a long patch of bottom ripples (amplitude b , wavenumber \mathbf{k}_b). Because of third-order interactions, the surface wave amplitudes vary slowly with time t : $a_n(\tau)$, $n = 1, 2, 3$ where $\tau = \epsilon^2 t$ and $\epsilon \ll 1$ is a measure of surface steepness. The total energy density per unit area given by $E_0 = \rho g(a_1^2 + a_2^2 + a_3^2)/2$ is constant in time (ρ and g are the water density and gravitational acceleration, respectively). Hence,

$$a_1 \frac{da_1}{d\tau} + a_2 \frac{da_2}{d\tau} + a_3 \frac{da_3}{d\tau} = 0. \quad (3.1)$$

Therefore we have, in general,

$$\frac{da_1}{d\tau} = \alpha_1 a_2 a_3, \quad \frac{da_2}{d\tau} = \alpha_2 a_1 a_3, \quad \frac{da_3}{d\tau} = \alpha_3 a_1 a_2. \quad (3.2)$$

where the growth rates α_n , $n = 1, 2, 3$ are constants with $\alpha_1 + \alpha_2 + \alpha_3 = 0$. These coefficients can be derived from regular perturbation solution at the third order. The derivation is lengthy but standard by now and is omitted. The coefficient of the resonant wave is $\alpha_3 \equiv \alpha_r = b(P \cosh k_r h - gQ)/(2g \cosh k_r h)$ where

$$P = \sum_{i=1,2} A_{jib} k_{jb} \left\{ \frac{1}{2} g^2 \left(k_{jb}^2 + \frac{\omega_j}{\omega_i} k_i^2 \right) - \frac{1}{2} \omega_j (\omega_i^3 + \omega_j^3) + [g^2 (\mathbf{k}_i \cdot \mathbf{k}_{jb}) - \omega_i^2 \omega_j^2] \left(1 + \frac{\omega_j}{\omega_i} \right) \right\}, \quad (3.3)$$

$$Q = A_{12} [(\mathbf{k}_1 + \mathbf{k}_2) \cdot \mathbf{k}_r] / 2, \quad (3.4)$$

where $j = 2, 1$ respectively when $i = 1, 2$, and

$$A_{12} = -M / [\cosh k_{12} h (\omega_{12}^2 - g k_{12} \tanh k_{12} h)],$$

$$A_{ib} = N_i / [k_{ib} \cosh k_{ib} h (\omega_i^2 - g k_{ib} \tanh k_{ib} h)], \quad (3.5)$$

$$N_i = \frac{g (\mathbf{k}_i \cdot \mathbf{k}_{ib})}{2\omega_i \cosh k_i h}, \quad i = 1, 2, \quad (3.6)$$

$$M = g^2 \frac{\omega_1 k_2^2 + \omega_2 k_1^2 + 2(\mathbf{k}_1 \cdot \mathbf{k}_2)(\omega_1 + \omega_2)}{2\omega_1 \omega_2} - \omega_1 \omega_2 (\omega_1 + \omega_2) - (\omega_1^3 + \omega_2^3) / 2. \quad (3.7)$$

Here $\mathbf{k}_{12} = \mathbf{k}_1 + \mathbf{k}_2$, $\omega_{12} = \omega_1 + \omega_2$, $\mathbf{k}_{ib} = \mathbf{k}_i + \mathbf{k}_b$ for $i = 1, 2$, $\mathbf{k}_r = \mathbf{k}_1 + \mathbf{k}_2 + \mathbf{k}_b$ and $\omega_r = \omega_1 + \omega_2$. Coefficients α_1 and α_2 are similarly obtained by permutating \mathbf{k}_1 , \mathbf{k}_2 and \mathbf{k}_r in the above equations.

The coefficient α_r measuring the strength of the resonance depends linearly on the bottom ripple amplitude; and nonlinearly on the participant wave frequencies/wavenumbers as well as the direction of the wavenumbers of the interacting components. Figure 2 shows the dependence of α_r on θ_{21} and θ_{r1} . Figure 2 shows that for sub(superharmonic) class III resonance, the largest growth rate occurs when \mathbf{k}_1 , \mathbf{k}_2 (\mathbf{k}_1 , \mathbf{k}_r) are (nearly) aligned. This general behaviour is found to obtain over broad ranges of the underlying parameters.

The solution to (3.2) can be written in terms of Jacobi elliptic functions. Assuming initial amplitudes $a_{10}, a_{20} \neq 0$ and $a_{30} = 0$, we have two solution cases: (i) $\alpha_1 \alpha_2 > 0$; and (ii) $\alpha_2 \alpha_3 > 0$. For case (i), we define $m = a_{10}/a_{20} \sqrt{\alpha_2/\alpha_1}$. If $m \geq 1$, then

$$a_1(\tau) = -a_{10} \operatorname{cn}(\gamma\tau), \quad a_2(\tau) = a_{20} \operatorname{dn}(\gamma\tau), \quad a_3(\tau) = a_{10} \sqrt{-\alpha_3/\alpha_1} \operatorname{sn}(\gamma\tau), \quad (3.8)$$

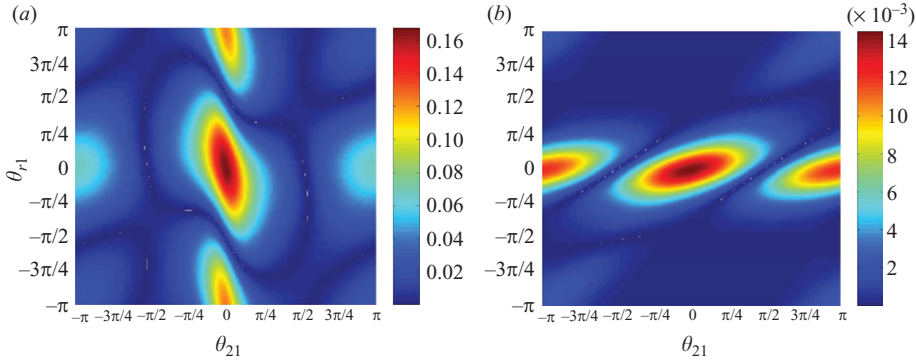


FIGURE 2. Dimensionless growth rate $\alpha_r(b\sqrt{g/h^5})^{-1}$ as a function of θ_{21} and θ_{r1} for: (a) subharmonic and (b) superharmonic resonance; for fixed $k_1h = 3.13$, $k_2h = 2.06$ (therefore $k_rh = 0.364$).

where $\gamma = a_{10}\sqrt{-\alpha_2\alpha_3}/m = a_{20}\sqrt{-\alpha_1\alpha_3}$, and m is the modulus of the elliptic function. From (3.8), it is seen that the amplitude of the resonant wave has a maximum of $a_{3,max} = a_{10}\sqrt{-\alpha_3/\alpha_1}$. If $m < 1$, then

$$a_1(\tau) = -a_{10} \operatorname{dn}(\gamma\tau), \quad a_2(\tau) = a_{20} \operatorname{cn}(\gamma\tau), \quad a_3(\tau) = a_{10}/m \sqrt{-\alpha_3/\alpha_1} \operatorname{sn}(\gamma\tau), \quad (3.9)$$

where $\gamma = a_{10}\sqrt{-\alpha_2\alpha_3} = ma_{20}\sqrt{-\alpha_1\alpha_3}$, and now $1/m$ is the modulus of the elliptic function. One interesting case is when $m = 1$. In this case, after some finite time, the amplitudes of the two initial waves vanish and the amplitude of the resonant wave reaches a finite value. Since no subsequent interactions occur, the constant-amplitude resonant wave is the only wave that remains after this time.

For case (ii), $\alpha_2\alpha_3 > 0$, then

$$a_1(\tau) = -a_{10} \operatorname{sn}\varphi, \quad a_2(\tau) = a_{20}/\cos\beta \operatorname{dn}\varphi, \quad a_3(\tau) = a_{10}\sqrt{-\alpha_3/\alpha_1} \operatorname{cn}\varphi, \quad (3.10)$$

where $\varphi = \gamma\tau - K$ and K is the complete elliptic integral of the first kind, i.e. $\operatorname{sn}K = 1$. We define $m = \sin\beta$ where $\tan^2\beta = (a_{10}/a_{20})^2(-\alpha_2/\alpha_1)$, then $\gamma = a_{20}\sqrt{-\alpha_1\alpha_3}/\cos\beta = -a_{10}\sqrt{\alpha_2\alpha_3}/\sin\beta$. This last solution is also given by Ball (1964) for triad resonance between surface and interfacial waves. In all cases studied above, the period of amplitude modulation is $\tilde{T} = 4K/\gamma$. It can be shown that $a_{r,max}$ does not depend on the direction of propagation of waves, therefore, the frequency of modulation of amplitudes γ follows the same pattern as that of the growth rate in figure 2(a, b).

4. Numerical results

To illustrate the features of sub- and super-harmonic Class III Bragg resonance, we consider selected scenarios using the theoretical solution of §3 and direct numerical simulation (Liu & Yue 1998). The latter is a high-order (pseudo) spectral (HOS) method originally developed for nonlinear wave-wave interactions (Dommermuth & Yue 1987), and later extended to include bottom undulations (Liu & Yue 1998).

The direct numerical simulation uses periodic boundary conditions and considers the time evolution of the wave amplitudes (the results can be interpreted in terms of spatial evolution of the same, see Liu & Yue 1998). In the simulations, we use a rectangular domain of $L_x \times L_y$, $N_x \times N_y$ Fourier wave modes, and $N_t = T_1/\delta t$ (fourth-order Runge-Kutta) time steps per period of the k_1 incident wave. In all

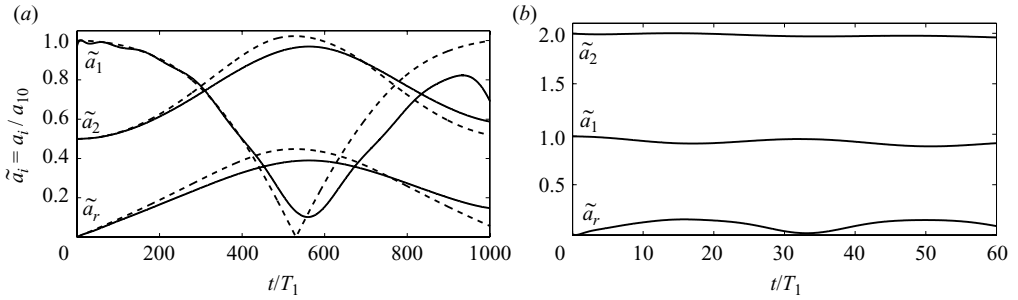


FIGURE 3. Evolution of amplitudes of incident and subharmonic class III Bragg resonant waves: (a) two copropagating surface waves $k_{1,2}h = 3.13, 2.06$ (initial steepnesses $\epsilon_{1,2} = 0.09, 0.03$) over a bottom ripple with $k_b h = 0.71$ ($\epsilon_b = 0.08$) resonate a transmitted wave of $k_r h = 0.36$. The amplitudes plotted are $\tilde{a}_i = a_i/a_{10}$, $i = 1, 2, r$. The HOS results (—, obtained with $L_x = 172\lambda_1$, $N_x = 2048$, $N_t = 32$) are compared with perturbation predictions (- - -) of § 3. (b) Resonance of two counter-propagating surface waves $k_{1,2}h = 2.02, 1.33$ ($\epsilon_{1,2} = 0.1, 0.13$) over a bottom ripple with $k_b h = 3.03$ ($\epsilon_b = 0.37$), resonate a subharmonic wave of $k_r h = 0.32$. The HOS results (—) are obtained with $L_x = 100\lambda_1$, $N_x = 2048$, $N_t = 32$.

the simulations below, we use nonlinear order $M = 4$. For the parameters used, the numerical results are typically converged to $< O(1\%)$ (see Liu & Yue 1998, for extensive convergence tests and validations).

4.1. Subharmonic resonance in normal incidence

Any copropagating wave pairs $(k_1, \omega_1), (k_2, \omega_2)$ in an incident wave spectrum that satisfy $\mathcal{F}(|\omega_1 - \omega_2|) = |k_1 - k_2| - k_b$ are in resonance with a subharmonic wave $(k_r, \omega_r) = (|k_1 - k_2| - k_b, |\omega_1 - \omega_2|)$. For near-shore sandbars of typical wavelength $\lambda_b = O(10-100)$ m (see e.g. Mei, Stiassnie & Yue 2005; Yu & Mei 2000b), this mechanism can transfer energy from short incident waves to resonant reflected and transmitted waves of $O(10)$ times greater wavelength. Figure 3(a) shows numerical results for such a case compared to the perturbation predictions (§ 3). The amplitudes show the growth/decrease and subsequent modulations as energy is exchanged among the three resonant interacting waves. The perturbation theory and HOS compare well initially but eventually deviate after long time as other (near resonant and non-resonant) nonlinear interactions enter the numerical simulation. For $h = 5$ m, say, the parameters in figure 3(a) correspond to $\lambda_b = 44$ m, $\lambda_{1,2} = 10, 15$ m and $\lambda_r = 86$ m. At $t/T_1 \sim 100$, when $a_r \sim 0.3a_{r,max}$ ($a_{r,max} \sim 0.4a_{10}$ for $\epsilon_b = 0.08$ say), the resonant wave has propagated over a distance of $\sim 38\lambda_b$; while at peak modulation (maximum a_r) $t/T_1 \sim 500$, this corresponds to a bottom patch of $\sim 185\lambda_b$, which is probably unrealistic.

In the presence of (partial) reflection at the shore, counter-propagating waves (of different frequencies) may be present and participate in resonance interactions with the bottom (e.g. Yu & Mei 2000a). The presence of (generalized) Bragg resonance reflections themselves offers additional mechanisms for such scenarios (for instance, if $k_b h = 1.43$ in figure 3(a) with the same incident waves, a subharmonic resonant wave of the same wavelength would be reflected). Figure 3(b) shows a class III subharmonic resonance due to a pair of counter-propagating surface waves. Compared with figure 3(a), the amplitude and period of modulations are smaller. In dimensional terms for $h = 30$ m say, the parameters in figure 3(b) correspond to $\lambda_b = 63$ m, $\lambda_{1,2} = 94, 143$ m and $T_r = 34.7$ s, $\lambda_r = 586$ m which is in the (shorter) range of typical

infragravity waves. Such low frequency long waves may be of practical and significant concern to mooring of coastal vessels (e.g. Renaud *et al.* 2008).

From the theoretical results, (3.2), it can be shown that for the conditions of figure 3(a) the initial growth rate α_r and frequency of amplitude modulation γ of the resonance generated subharmonic wave for co-propagating incident waves are an order of magnitude higher than those for counter-propagating incident waves. This can be seen from figure 2(a) for the subharmonic case, in which the magnitude of α_r for $\theta_{21} = 0$ and $\theta_{r1} = 0$ is much larger than that for θ_{21} close to π .

4.2. Oblique subharmonic resonance of longshore waves

The origin of infragravity waves in the power spectra in inner surf zones has been a matter of dispute (Munk 1949; Huntley 1976; Lippmann, Holman & Bowen 1997; Henderson *et al.* 2006). Field measurements have shown that these waves are predominantly longshore (Herbers, Elgar & Guza 1995). Leading order bottom effects are known to be important in the scattering of these waves (Chen & Guza 1999).

We show here how class III subharmonic resonance can generate long longshore waves due to a pair of incident waves (slightly) oblique to the bottom ripples. Consider a pair of waves incident at an oblique angle θ_{b1} relative to \mathbf{k}_b . If $\mathcal{F}(|\omega_1 - \omega_2|) = k_b \tan \theta_{b1}$, a subharmonic longshore wave of $k_r = |k_1 - k_2| \sin \theta_{b1} = k_b \tan \theta_{b1}$ is generated. Figure 4 shows the amplitude evolutions and (instantaneous) wave pattern corresponding to such a scenario for $\theta_{b1} = 0.3$ with $k_r/k_1 \approx 0.1$. Relative to figure 3 case, the strength of the (initial) resonance growth is stronger than figure 3(a) and substantially so compared to the counter-propagating case. This trend is consistent with the theoretical value of the growth rate coefficient, $\alpha_r = \alpha_3$ in (3.2), and is a result of the choice of shorter initial waves compared to figure 3. In fact, it can be shown from (3.2) that for the same incident wave parameters and depth, the growth rate of the resonant wave in oblique incidence is generally smaller than that in normal incidence. The wave pattern (figure 4b) shows the short-crested wave feature due to the modulation by the longshore waves. In physical terms, for $h = 30$ m, $\lambda_b = 94$ m, $\lambda_{1,2} = 42, 78$ m and $\lambda_r = 304$ m propagating parallel to the bottom contours.

4.3. Oblique superharmonic resonance of standing-propagating waves

Incident waves can, on occasion, propagate parallel to the shoreline (e.g. Herbers *et al.* 1995), and, as we suggest in §4.2, possibly from class III oblique resonance. We show here that a pair of shore parallel propagating waves can generate Bragg resonance waves that are oblique to the bottom ripples via a class III superharmonic mechanism. Consider two incident waves ($\mathbf{k}_i, i = 1, 2$) propagating perpendicular to the bottom ripples $\mathbf{k}_b, \mathbf{k}_i \cdot \mathbf{k}_b = 0$. If $\mathbf{k}_1, \mathbf{k}_2$ satisfy $\mathcal{F}(\omega_1 + \omega_2) = |\mathbf{k}_1 + \mathbf{k}_2 + \mathbf{k}_b|$, two superharmonic oblique resonance waves given by $(\mathbf{k}_r^\pm, \omega_r) = (\mathbf{k}_1 + \mathbf{k}_2 \pm \mathbf{k}_b, \omega_1 + \omega_2)$ are generated with $\theta_{r1}^\pm = \pm \arctan[k_b/(k_1 + k_2)]$ (by symmetry, figure 1b with $\mathbf{k}_i \perp \mathbf{k}_b$). Since there is no preferred direction, energy equally distributes between the \mathbf{k}_r^\pm resonant waves resulting in a standing-propagating wave in the shore normal-parallel directions. Figure 5 shows such a case with $k_2/k_1 = 0.63, k_b/k_1 = 1.49$; and superharmonic $k_r/k_1 = 2.21$ with $\theta_{r1}^\pm = \pm 0.74$. The amplitude a_r grows monotonically initially while a_1 and a_2 oscillate and decrease. The resonance is relatively strong and $a_r/a_{10} \sim 20\%$ after $t/T_1 = 50$. The instantaneous free surface (figure 5b) show a (longshore propagating) egg-crate feature, characteristic of a standing-propagating wave (say, created by a perfectly reflected oblique wave). The physical parameters for figure 5 are not unrealistic (Mei *et al.* 2005): for example, for $h = 24$ m, $\lambda_b = 100$ m, $\lambda_{1,2} = 240, 150$ m ($T_{1,2} = 16.6, 11.2$ s), and \mathbf{k}_r is superharmonic with $T_r = 6.7$ s and $\lambda_r = 68$ m. Note that the resonant standing wave has a shore-normal wavelength equal to λ_b . Such

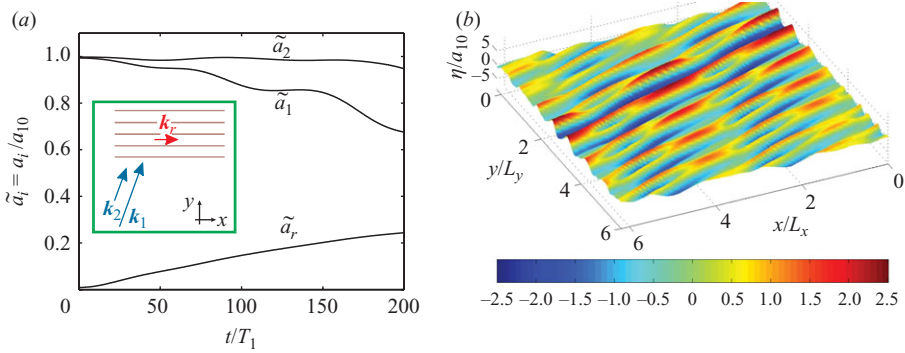


FIGURE 4. (a) Evolution of amplitudes of incident and resonant waves in an oblique class III Bragg resonance. A longshore wave ($k_r h = 0.6$) formed as a result of a subharmonic class III Bragg resonance (§4.2) between two copropagating incident waves $k_{1,2} h = 4.5, 2.4$ ($\epsilon_{1,2} = 0.24, 0.13$) with $\theta_{1b} = \theta_{2b} = 0.3$ with respect to a bottom of $k_b h = 2.01$ ($\epsilon_b = 0.40$). Simulation parameters are $N_x = 128$, $N_y = 64$, $N_t = 32$ and $L_x = L_y = 15\lambda_1$. (b) A surface snapshot at $t/T_1 = 200$.

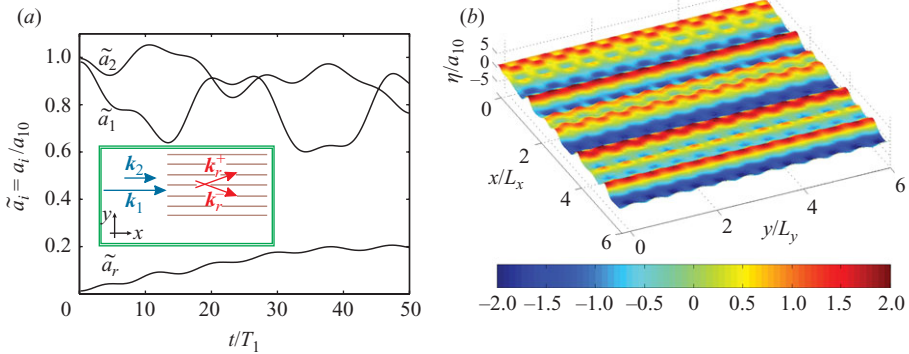


FIGURE 5. (a) Evolution of amplitudes of incident and resonant waves corresponding to oblique superharmonic class III Bragg resonance (§4.3): two copropagating longshore waves $k_{1,2} h = 1.00, 0.63$ ($\epsilon_{1,2} = 0.08, 0.05$) over a bottom of $k_b h = 1.49$ ($\epsilon_b = 0.48$) excite two resonate waves $k_r h = 2.21$ propagating obliquely ($\theta_{r1}^\pm = \pm 0.74$) with respect to the incident wave angle. Simulations parameters are $N_x = 128$, $N_y = 64$, $L_x = L_y = 8\lambda_1$ and $N_t = 16$. (b) A surface snapshot at $t/T_1 = 50$.

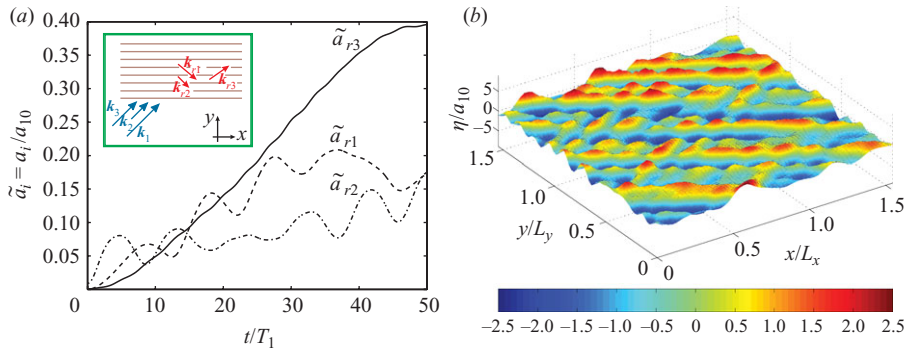


FIGURE 6. Direct simulation of multiple Bragg resonance initially involving three (copropagating) oblique incident waves and three bottom ripple components: (a) evolution of the amplitudes of first three oblique class III Bragg resonant waves, and (b) a snapshot of the wave surface after $t/T_1 = 50$ (only a portion of the simulation domain is shown). The numerical simulation uses $L_x = L_y = 50\lambda_1$, $N_x = N_y = 512$ and $N_t = 16$. The initial steepnesses are $\epsilon_{1,2,3,b1,b2,b3} = 0.04, 0.02, 0.01, 0.11, 0.17, 0.05$.

shore-normal standing waves likely contribute to the formation/deformation of sandbars (Yu & Mei 2000*b*; Landry, Hancock & Mei 2007; Hancock, Landry & Mei 2008).

4.4. Multiple resonances

In the most general context, ocean surface waves and bottom undulations contain many frequency and wavenumber components participating in multiple Bragg resonances resulting in resonant waves which themselves satisfy Bragg resonance conditions. Such a scenario is analytically intractable over time but ideally suited to direct simulations such as HOS.

Figure 6 shows such a result highlighting the role of (oblique) class III interactions in the multiple Bragg resonances. The simulation is set up initially with three co-propagating incoming waves, $k_{1,2,3}h = 1, 0.3, 0.5$ obliquely incident with $\theta_{b1} = 0.57$ containing three wavenumber components $k_{b1,b2,b3}h = 1.06, 0.72, 0.34$. With these values, two separate quartet interactions immediately obtain with (obliquely) reflected $k_{r1}h = 0.60$, $\theta_{r1} = 2.5$ due to \mathbf{k}_1 , \mathbf{k}_2 and \mathbf{k}_{b1} , and $k_{r2}h = 0.40$, $\theta_{r2} = 2.4$ due to \mathbf{k}_1 , \mathbf{k}_3 and \mathbf{k}_{b2} . After some time, \mathbf{k}_{r1} , \mathbf{k}_{r2} and \mathbf{k}_{b3} form a resonant quartet with a new transmitted wave component $k_{r3}h = 0.20$, $\theta_{r3} = 0.58$ which is (almost) parallel to $\mathbf{k}_{1,2,3}$. The multiple resonances then continue. In figure 6(a), we focus on the evolutions of the first three quartet resonant waves (only) showing the (modulated) growth of these amplitudes. In this case, the amplitude of modulation of a_{r3} (which has zero slope initially) is greater than those of a_{r1} , a_{r2} , so that $a_{r3} > a_{r1}, a_{r2}$ after relatively short time $t/T_1 \gtrsim 20$; and $a_{r3,max} \sim 0.4a_{10}$ at $t/T_1 \sim 50$. Figure 6(b) shows the instantaneous free surface at that time, where much of the coherence is lost.

5. Conclusion

We consider oblique quartet (third-order) class III Bragg resonance interaction of three surface wave with one bottom ripple component. Unlike class I and II Bragg resonances (involving two monochromatic surface and respectively one and two bottom components), class III resonance occurs at the sum and difference of the incident wave frequencies with wavenumber vectors that can vary broadly depending on the problem. We study the general problem, considering theoretically the resonance condition and the amplitude evolution. These are complemented by direct numerical simulation using a high-order spectral methods.

Real ocean surface is composed of a spectrum of wave frequencies (and directions). Bottom topography likewise may contain multiple wavenumbers. Oblique sub/super-harmonic class III resonances offer important mechanisms for wave energy transfer in frequency and direction. We show, using illustrative cases, such scenarios. These include subharmonic shore-normal transmissions for normal incident waves, subharmonic long longshore wave generation for oblique incident waves, and superharmonic standing-propagating waves due to longshore incident waves. Finally, we consider a case of multiple Bragg resonance where class III interactions play a critical role. Our considerations suggest that, under specific but realistic conditions involving bottom ripples, class III energy transfer across the frequency-directional wave spectrum can be significant, with potential implications to coastal engineering and the study of near-shore processes. We finally note that the generation, growth and modulation of class III Bragg resonant waves would, in general, be affected by other physical phenomena such as wave breaking and bottom dissipation which are not considered here.

This research is supported financially by grants from the Office of Naval Research.

REFERENCES

- ARDHUIN, F. & HERBERS, T. H. C. 2002 Bragg scattering of random surface gravity waves by irregular seabed topography. *J. Fluid Mech.* **451**, 1–33.
- ARDHUIN, F. & MAGNE, R. 2007 Scattering of surface gravity waves by bottom topography with a current. *J. Fluid Mech.* **576**, 235–264.
- BABCOCK, J. M., KIRKENDALL, B. A. & ORCUTT, J. A. 1994 Relationships between ocean bottom noise and the environment. *Bull. Seismol. Soc. Am.* **84** (6), 1991–2007.
- BALL, F. 1964 Energy transfer between external and internal gravity waves. *J. Fluid Mech.* **19**, 465–478.
- CHEN, Y. & GUZA, R. T. 1999 Resonant scattering of edge waves by longshore periodic topography: finite beach slope. *J. Fluid Mech.* **387**, 255–269.
- DAVIES, A. G. 1982 The reflection of wave energy by undulation on the seabed. *Dyn. Atmos. Oceans* **6**, 207–232.
- DAVIES, A. G. & HEATHERSHAW, A. D. 1984 Surface-wave propagation over sinusoidally varying topography. *J. Fluid Mech.* **144**, 419–443.
- DOMMERMUTH, D. G. & YUE, D. K. P. 1987 A higher-order spectral method for the study of nonlinear gravity waves. *J. Fluid Mech.* **184**, 267–288.
- ELGAR, S., RAUBENHEIMER, B. & HERBERS, T. H. C. 2003 Bragg reflection of ocean waves from sandbars. *Geophys. Res. Lett.* **30** (1), 1016.
- GUZZELLI, E., REY, V. & BELZONS, M. 1991 Higher-order Bragg reflection of gravity surface waves by periodic beds. *J. Fluid Mech.* **245**, 301–317.
- HANCOCK, M. J., LANDRY, B. J. & MEI, C. C. 2008 Sandbar formation under surface waves: theory and experiments. *J. Geophys. Res.* **113**, C07022.
- HARA, T. & MEI, C. C. 1987 Bragg scattering of surface waves by periodic bars: theory and experiment. *J. Fluid Mech.* **178**, 221–241.
- HEATHERSHAW, A. D. 1982 Seabed-wave resonance and sand bar growth. *Nature* **296** (5855), 343–345, 10.1038/296343a0.
- HEATHERSHAW, A. D. & DAVIES, A. G. 1985 Resonant wave reflection by transverse bedforms and its relation to beaches and offshore bars. *Mar. Geol.* **62**, 321–338.
- HENDERSON, S. M., GUZA, R. T., ELGAR, S., HERBERS, T. H. C. & BOWEN, A. J. 2006 Nonlinear generation and loss of infragravity wave energy. *J. Geophys. Res.* **111**.
- HERBERS, T. H. C., ELGAR, S. & GUZA, R. T. 1995 Generation and propagation of infragravity waves. *J. Geophys. Res.* **100** (C12), 24,863–24,872.
- HUNTLEY, D. A. 1976 Long-period waves on a natural beach. *J. Geophys. Res.* **81** (36), 6441–6449.
- KIRBY, J. T. 1986 A general wave equation for waves over rippled beds. *J. Fluid Mech.* **162**, 171–186.
- LANDRY, B. J., HANCOCK, M. J. & MEI, C. C. 2007 Note on sediment sorting in a sandy bed under standing water waves. *Coast. Engng* **54** (9), 694–699, doi: 10.1016/j.coastaleng.2007.02.003.
- LIPPMANN, T. C., HOLMAN, R. A. & BOWEN, A. J. 1997 Generation of edge waves in shallow water. *J. Geophys. Res.* **102** (C4), 8663–8679.
- LIU, Y. & YUE, D. K. P. 1998 On generalized Bragg scattering of surface waves by bottom ripples. *J. Fluid Mech.* **356**, 297–326.
- MADSEN, P. A. & FUHRMAN, D. R. 2006 Third-order theory for bichromatic bi-directional water waves. *J. Fluid Mech.* **557**, 369–397.
- MEI, C. C. 1985 Resonant reflection of surface water waves by periodic sandbars. *J. Fluid Mech.* **152**, 315–335.
- MEI, C. C., HARA, T. & NACIRI, M. 1988 Note on Bragg scattering of water waves by parallel bars on the seabed. *J. Fluid Mech.* **186**, 147–162.
- MEI, C. C., STIASSNIE, M. & YUE, D. K.-P. 2005 *Theory and Applications of Ocean Surface Waves. Part 1,2, Advanced Series on Ocean Engineering*, vol. 23. World Scientific.
- MUNK, W. H. 1949 Surf beats. *EOS Trans. AGU* **30**, 849–854.

- NACIRI, M. & MEI, C. C. 1988 Bragg scattering of water waves by a doubly periodic seabed. *J. Fluid Mech.* **192**, 51–74.
- PORTER, R. & PORTER, D. 2001 Interaction of water waves with three-dimensional periodic topography. *J. Fluid Mech.* **434**, 301–335.
- RENAUD, M., REZENDE, F., WAALS, O., CHEN, X. B. & VAN DIJK, R. 2008 Second-order wave loads on a lng carrier in multi-directional waves. In *Proceeding of OMAE 2008, 26th international Conference on Offshore Mechanics and Arctic Engineering, June 2008*, Estoril, Portugal.
- YU, J. & MEI, C. C. 2000a Do longshore bars shelter the shore? *J. Fluid Mech.* **404**, 251–268.
- YU, J. & MEI, C. C. 2000b Formation of sand bars under surface waves. *J. Fluid Mech.* **416**, 315–348.